JCTC Journal of Chemical Theory and Computation

Calculating Reaction Rates with Partial Hessians: Validation of the Mobile Block Hessian Approach

A. Ghysels, V. Van Speybroeck, T. Verstraelen, D. Van Neck, and M. Waroquier*

Center for Molecular Modeling, Ghent University, Proeftuinstraat 86, B-9000 Gent, Belgium

Received October 24, 2007

Abstract: In an earlier paper, the authors have developed a new method, the mobile block Hessian (MBH), to accurately calculate vibrational modes for partially optimized molecular structures [*J. Chem. Phys.* **2007,** *126* (22), 224102]. The proposed procedure remedies the artifact of imaginary frequencies, occurring in standard frequency calculations, when parts of the molecular system are optimized at different levels of theory. Frequencies are an essential ingredient in predicting reaction rate coefficients due to their input in the vibrational partition functions. The question arises whether the MBH method is able to describe the chemical reaction kinetics in an accurate way in large molecular systems where a full quantum chemical treatment at a reasonably high level of theory is unfeasible due to computational constraints. In this work, such a validation is tested in depth. The MBH method opens a lot of perspectives in predicting accurate kinetic parameters in chemical reactions where the standard full Hessian procedure fails.

1. Introduction

Ab initio prediction of reaction rate constants of chemical reactions has a high computational cost, especially when large (bio)molecular systems are involved. An accurate description of chemical kinetics of reactions in gas phase is nowadays perfectly practicable for moderate-sized molecules, but once the molecular environment comes into play, one has to adapt the level of theory in such way to make the computation feasible.[1] This puts a heavy burden on the accuracy of the numerical results. Chemical kinetics in static approaches is still widely based on transition state theory (TST).[2–5] Key parameters are the reaction energy barrier between the reactants and activated complex (the transition state) and the vibrational frequencies, which serve as an input in the partition functions, and their accurate computation is essential. In the molecular-statistical formulation of TST, they completely determine the equilibrium constant by the use of partition functions.

In the harmonic oscillator approximation, the molecular partition function is factorized in a translational, rotational, and vibrational contribution, where the latter is completely determined by the eigenfrequencies. Frequencies are usually computed by a normal-mode analysis (NMA). This is the main bottleneck in ab initio predictions of chemical kinetics in large molecular systems, since frequency calculations are computationally very demanding even if analytical second derivatives are employed, rather than numerical ones. If a molecular mechanics (MM) force field is used instead of a quantum mechanics (QM) or hybrid (QM/MM)[6–9] description, the frequency calculation becomes less problematic, though even at the full MM level other issues, such as the storage and manipulation of the huge Hessian matrices associated with very large systems, can become prohibitive in real applications. Anyway, chemical reactions inherently involve bond breaking and charge transfer; so, it is essential to provide a QM description for (at least) the reactive region and a full MM description is usually no option.

In addition, there are computational limitations in the geometry optimization of extended systems at a high level of theory (LOT). Very often one goes over to a partial optimization: the interesting region containing the active site is optimized at a high LOT, while the environment is kept fixed at a low LOT geometry. This approach permits one to obtain an ab initio description of the chemically active site

* Corresponding author. E-mail: michel.waroquier@UGent.be.

10.1021/ct7002836 CCC: $40.75
Published on Web 02/27/2008

in large molecular systems, but at the same time, it creates several new problems. One of them is the extraction of accurate frequencies for the relevant vibrational modes. All partially optimized systems are nonequilibrium structures, and as a consequence of the residual gradients on the potential energy surface (PES), the standard full Hessian normal-mode analysis may show some unphysical results, e.g., spurious imaginary frequencies may appear. A frequency analysis in terms of a subset of coordinates that are optimized, i.e. a partial Hessian method, can avoid these problems.

The authors have succeeded recently in deriving a method that is able to calculate physical frequencies. The main idea is to group the atoms that were kept fixed during the partial optimization into one or more blocks that are able to move as rigid bodies with respect to the relaxed molecular part in the vibrational analysis.[10] This mobile block Hessian (MBH) method has shown to be very efficient for an accurate evaluation of relevant frequencies of vibrational modes. The proposed procedure remedies the artifact of imaginary frequencies occurring in standard frequency calculations for partially optimized systems. In addition, only a subblock of the Hessian matrix has to be constructed and diagonalized, leading to a serious reduction of the computation time for the frequency analysis.

MBH can be regarded as an extension of the partial Hessian vibrational analysis approach (PHVA). Only part of the cartesian Hessian has been retained, excluding all the atoms of the passive site of the molecule that is kept fixed during the optimization. This methodology was first introduced and developed by Head and co-workers[11–14] and was further investigated by Li and Jensen[15] and Besley and Metcalf.[16] It comes to giving an infinite mass to the fixed atoms so that they are frozen at their initial position. Only the relaxed atoms can participate in the small amplitude vibrations.

The novelty of MBH with respect to PHVA lies in the fact that, in the former, the finite mass of each block is taken into consideration in the NMA, instead of giving an infinite mass to the fixed atoms. Six degrees of freedom are attributed to each block to describe its position and orientation with respect to the fully optimized part, and the global translational/rotational invariance of the potential energy surface (PES) is fully respected. Moreover, the PHVA is always limited to the case of one immobile block with infinite mass, whereas in the MBH model, parts of the molecular system can be ranged in multiple blocks which can move as rigid bodies with respect to the relaxed part of the molecule. In ref 10, both PHVA and MBH methods are submitted to a tough comparative study, while in ref 17, attention is given to the practical implementation of the MBH model and the interface with molecular modeling program packages.

One of the main applications that can be deduced from the knowledge of accurate normal-mode frequencies, is the prediction of chemical kinetics, as already mentioned. By means of the partition functions and a molecular-statistical formulation of transition state theory, the reaction rate constant k of a chemical reaction can be determined.[2–5] A somewhat different approach is proposed by the group of Lin et al.[18] Basic assumption is that the Hessian elements that involve only the atoms of the active site might be more critical than the other Hessian elements. The less critical elements are approximated following some interpolation procedure, mainly for elements at the nonstationary points on the potential energy surface which are not consistently constructed by the same level (dual level scheme). Other related papers suggest proper methods to predict accurate QM/MM kinetics by incorporating quantum mechanical effects by treating vibrational motions quantum mechanically and applying multidimensional tunneling approximations into reaction rate calculations.[19,1] Recently, more sophisticated techniques concerning transition state theory have been developed including tunneling effects, quantum dynamical effects and multiple pathways (we refer to ref 20 for a review of all modern developments), but in view of the goal of this paper to validate the MBH approach in predicting kinetics, conventional TST largely suffices and tunneling and other effects will not be incorporated.

In principle, the expression of k includes all normal vibrational modes in reactants and activated complex. It is inherent to both MBH and PHVA approaches that the number of frequencies is always smaller than in a standard frequency calculation. The question arises whether this reduction has a significant influence on the reaction rate constant. Here lies the scope of this work: we will demonstrate that the normal modes which disappear when defining fixed blocks have little influence on the chemical kinetics. This work aims at promoting MBH as a suitable and highly efficient tool for predicting accurate chemical kinetics parameters in large extended molecular systems where the standard full Hessian procedure fails.

Applications of MBH are numerous. They can be classified in various categories:

(i) Large biosystems consisting of thousands of atoms require a hybrid quantum mechanical/molecular mechanical (QM/MM) approach.[6–9] The whole MM region can be taken up in one or multiple blocks.

(ii) A cluster description of zeolites or other periodic systems, such as lattices, requires fixed positions of border atoms to prevent collapse of the molecule during optimization.[21–23] This represents a particular situation of partial optimization.

(iii) Reactions in solvents often require an approach with a chemical reactive site and various layers treated at different levels of theory (QM/MM or QM/QM′). The whole can even be circumvented by a bulk solvent described by a polarizable continuum model (PCM).[24,25] In MBH, the various solvent molecules are all regarded as mobile blocks which can translate and rotate freely around the active site. Only the internal structure of each solvent molecule is held fixed.

The structure of the paper is as follows. In section 2, a short outline of the theoretical methodology is given, and in section 3, the computational details are summarized. Section 4 is devoted to the validation of MBH as an adequate method to predict rate constants. Different reactions with various block choices are taken up in the test set for validation with the benchmark values (full optimization before frequency calculation). The test set includes a prototype substitution reaction, a hydrogen transfer reaction, as well as several

radical addition reactions, since these have a localized reactive site. The effectiveness of the multiple MBH has been illustrated with a more extended aminophosphonate system in section 4.3, for which solvent molecules are taken into account. The results of the MBH have been compared to those of the PHVA approach as well, and based on theoretical considerations, a modified PHVA method is presented in section 4.4, hereafter referred to as PHVA*. Finally in section 5, some conclusions are drawn.

2. Theoretical Background

2.1. Partition functions. Within the harmonic oscillator approximation, the $3N$ degrees of freedom of a N-atom system can be decoupled into three groups of independent motions—3 translational, 3 rotational, and $3N - 6$ vibrational motions—that all contribute to the total partition function Q:

$$Q = qq_{\text{elec}} \tag{1}$$

where

$$q = q_{\text{trans}}q_{\text{rot}}q_{\text{vib}} \tag{2}$$

The translational partition function reads

$$q_{\text{trans}} = \left(\frac{2\pi Mk_{\text{B}}T}{h^2}\right)^{3/2} V \tag{3}$$

M stands for the total mass of the system, T is the temperature, k_{B} is the Boltzmann constant, h is the Planck constant, and V is the volume. If I_1, I_2, and I_3 denote the moments of inertia of the system and σ is the symmetry number, the rotational partition function reads

$$q_{\text{rot}} = \frac{8\pi^2}{\sigma}\left(\frac{2\pi k_{\text{B}}T}{h^2}\right)^{3/2}\sqrt{I_1I_2I_3} \tag{4}$$

Each vibration with frequency ν_i, gives a contribution

$$q_{(\nu_i)} = \frac{e^{-h\nu_i/2k_{\text{B}}T}}{1 - e^{-h\nu_i/k_{\text{B}}T}} \tag{5}$$

to the total vibrational partition function

$$q_{\text{vib}} = \prod_i q_{(\nu_i)} \tag{6}$$

The electrons also contribute to the partition function, but when the first electronic excitation energy is much greater than $k_{\text{B}}T$, the first and higher excited states are assumed to be inaccessible. If E_0 is the energy of the ground-state level, this assumption simplifies the electronic partition function to

$$q_{\text{elec}} = e^{-E_0/k_{\text{B}}T} \tag{7}$$

Note that the zero point energy contribution $e^{-h\nu_i/2k_{\text{B}}T}$ in the numerator of eq 5 is frequently left out from the vibrational partition function and incorporated in the electronic partition function.

Ab initio molecular calculations can be used to generate the molecular properties required for the evaluation of the above partition functions, such as the geometry (for the moments of inertia I_i), the Hessian matrix (for the vibrational frequencies ν_i), and the electronic ground-state energy E_0.

2.2. Reaction Rate Constant within Conventional Transition State Theory (TST). Transition state theory has been proved to be very useful to determine the reaction rate constants.[2–5] It supposes that the transition state or activated complex is in equilibrium with the reactants, although, strictly speaking, this hypothesis is not valid since the transition state corresponds to a saddle point rather than a minimum on the PES. Within this assumption the rate constant is completely determined by the microscopic partition functions and the reaction barrier at 0 K.

For a unimolecular reaction, $A \rightarrow A^{\ddagger} \rightarrow B$ or $A \rightarrow A^{\ddagger} \rightarrow B + C$ (with the ‡ superscript indicating the activated complex) the rate constant k is given by:

$$k(T) = \frac{k_{\text{B}}T}{h}\frac{q(\ddagger)/V}{q(A)/V}e^{-\Delta E_0/k_{\text{B}}T} \tag{8}$$

ΔE_0 represents the molecular energy difference at 0 K between the activated complex and the reactants. The transition state frequency is assumed not to be included in the partition function $q(\ddagger)$ of the activated complex. k is expressed in units s^{-1}.

For a bimolecular reaction $A + B \rightarrow (AB)^{\ddagger} \rightarrow C$ or $A + B \rightarrow (AB)^{\ddagger} \rightarrow C + D$, the expression for the rate constant becomes

$$k(T) = \frac{k_{\text{B}}T}{h}\frac{q(\ddagger)/V}{q(A)/V\, q(B)/V}e^{-\Delta E_0/k_{\text{B}}T} \tag{9}$$

expressed in units of cubic meters per mole second.

2.3. MBH and PHVA. Partially optimized geometries are nonequilibrium structures. The usual normal-mode analysis (NMA) equations $H\nu = \omega^2 M\nu$, with H being the full cartesian Hessian and M the Cartesian diagonal mass matrix, could be solved to obtain the frequencies, but this procedure shows some serious defects. The Hessian H is the second derivative matrix of the potential energy with respect to all the Cartesian coordinates. At nonequilibrium geometries, it has only three zero-eigenvalues instead of six, implying that the rotational invariance of the potential energy surface is not manifest anymore.[26] Spurious imaginary frequencies appear. Moreover, the eigenvalues of the Hessian depend on the choice of coordinates.[27,28]

In the partial Hessian vibrational analysis (PHVA),[13,15] these defects are surmounted by giving the fixed atoms an infinite mass. The normal mode equations are then restricted to the relaxed atoms only, by taking a submatrix of the Hessian and the mass matrix:

$$H_{\text{E}}\nu = \omega^2 M_{\text{E}}\nu \tag{10}$$

The mobile block Hessian (MBH) model has been proposed recently by the authors[10] as an improvement of the PHVA. In the MBH model the fixed part is considered as a rigid body that is allowed to participate in the small amplitude vibrations, thus taking into account the finite mass of the fixed block. The spurious frequencies and the coordinate dependence are avoided since the system composed of optimized atoms plus block is in equilibrium. Relying on the global translational and rotational invariance, it is possible[10] to write the single block MBH normal mode equations in terms of the same submatrix H_{E} of the Hessian,

while the corresponding mass matrix is adapted because of the finite block mass:

$$H_E \nu' = \omega'^2 \tilde{M}' \nu' \quad (11)$$

with

$$\tilde{M}' = M_E - M_E D_E S^{-1} D_E^T M_E \quad (12)$$

The matrix D_E is constructed in terms of the coordinates of the free atoms with respect to a space fixed frame. The matrix S contains the information on the mass distribution, i.e. the total mass and the moments of inertia of the molecule. Details can be found in the Appendix and more extensively in ref 17.

The usefulness and applicability of the MBH approach are seriously increasing in case of extension to several mobile blocks. The multiple MBH takes into account the finite mass of each block, by including six parameters per block describing its position and orientation into the NMA equations and by mass weighting with the appropriate block mass and moments of inertia.

The multiple MBH method is for instance extremely useful when simulating chemical reactions in a solvent. Solvent molecules can easily be associated to rigid blocks with a fixed internal structure. They can move freely with respect to each other and with respect to the active site of the molecule.

At first sight the MBH is similar to the united atom concept in force fields, since groups of atoms are treated there also as a single entity.[29] However, in spite of this resemblance, the MBH is essentially different. In the MBH blocks each atom keeps its identity and continues to contribute individually to, e.g., moments of inertia, Hessian elements, steric hindrance, etc. Coarse-grained or united atom methods reduce the number of atoms and the initial all-atom potential energy surface is approximated by a parametrizized PES of lower dimension. The MBH on the other hand does not simplify the potential energy surface but freezes certain degrees of freedom when performing the vibrational analysis.

3. Computational Details

In order to validate both MBH and PHVA methods in their performance in reproducing accurate chemical kinetics, we compare the MBH and PHVA predictions for the reaction rate constant with benchmark values k.

Benchmark structures and frequencies are generated with a full geometry optimization at a high level of theory (DFT/B3LYP/6-311 g**) with tight convergence criteria such that the residual gradients on the PES are negligibly small. Consequently, a frequency calculation is carried out at the same level of theory for the whole molecular system. These equilibrium geometries permit to calculate the reaction rate with the full cartesian Hessian frequencies.

In a first analysis, frequencies and rate constants are calculated for the fully optimized geometry, while the block size is varied in the vibrational analysis. For each reaction under study, we take into consideration various choices of fixed blocks, or, various submatrices H_E of the Hessian. The normal mode equations, eqs 10 and 11, are constructed and solved using the same geometry, and thereby, any perturbation resulting from geometry differences is excluded in this particular treatment. This comparative study is thus highly appropriate to investigate the influence on the rate constants of exclusion of parts of the Hessian in the frequency calculation, i.e. limiting the NMA to a partial Hessian.

In a second analysis, partial geometry optimization is performed and consequently followed by a frequency calculation. For the MBH model, the position/orientation (six degrees of freedom) of each block are optimized, in contrary to PHVA, where the atoms in the single block are kept fixed in space. Therefore, a partial optimization with multiple blocks produces a better structure than one with a single block. We remind that PHVA is always limited to a single block, whereas MBH is very suitable to treat multiple blocks.

The partial optimization is performed as follows. First, one optimizes the system at a low level of theory (HF/STO-3g) to find a plausible starting structure. Then the rigid blocks are introduced and the system is partially optimized at a high level of theory (DFT/B3LYP/6-311 g**), while keeping the rigid blocks fixed at their initial internal geometry. All calculations were carried out with the Gaussian03 software package.[30] Next, a frequency calculation is performed with the second derivatives of the potential energy using the same high level of theory. The standard full Hessian frequency analysis would give unphysical results due to the residual forces present in the partial optimized structures, as mentioned in the Introduction. Instead, the PHVA or MBH normal mode eqs 10 and 11 are constructed, as these yield physical frequencies. Obviously, the same rigid blocks are chosen as those considered in the precedent partial optimization.

A partial Hessian method such as the MBH or PHVA approach, however, reduces the number of calculated frequencies. The difference in the number of degrees of freedom between reactants and transition state determines the temperature dependence of the reaction rate, as can be easily seen by inspecting eqs 8 and 9. This difference should not change when introducing the MBH blocks. It is therefore obvious that the chosen blocks must consist of the same atoms in reactant(s) and transition state. Note that strictly speaking the internal rigid block geometry might differ between reactants and transition state, because of the first step, i.e. optimization at the low level of theory before the actual partial optimization.

Finally, we made a selection of various chemical reactions for the validation. Most of them are radical addition reactions, but also one prototype substitution reaction (S_N2) and the hydrogen abstraction of one of the ending carbons are included (R6 and R7, respectively). In these reactions the reactive site (the radical center) is well localized. We choose addition reactions of ethene to a large variety of radicals with different substituents. It enables us to select various types of blocks (large and heavy blocks, substituents with ring structure(s), etc) and to give some recommendations in choosing the fixed blocks and the relaxed molecular region.

An overview of the different reactions under study is depicted in Figure 1. The reactions are labeled as R1, R2, etc. and the reactants and products are numbered. The block choices in the reactants are indicated and labeled in Figures

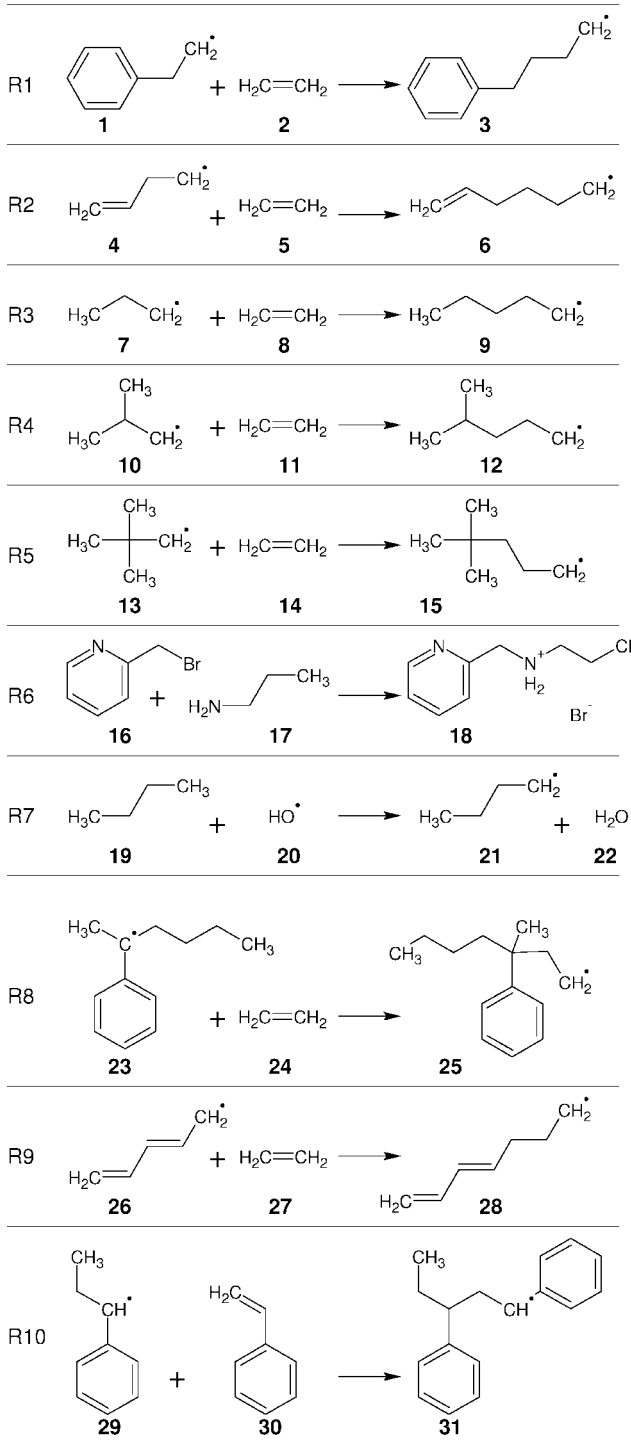

Figure 1. Overview of studied reactions.

2 and 3, and the transition state and product are assumed to contain the same block(s). Blocks can be classified in various types: they can include the reactive center (which at first view appears to be a surprising choice), they can directly be connected with the reactive center by a single bond, or they are separated by more than one bond. It is also possible to combine blocks to the case of multiple blocks. In bimolecular reactions, rigid blocks can be introduced in each of the two reactants; in the activated complex and product, they form multiple blocks, hindering in principle the application of the PHVA method. To illustrate, in reaction R10, one can combine blocks a and b in the description of the two

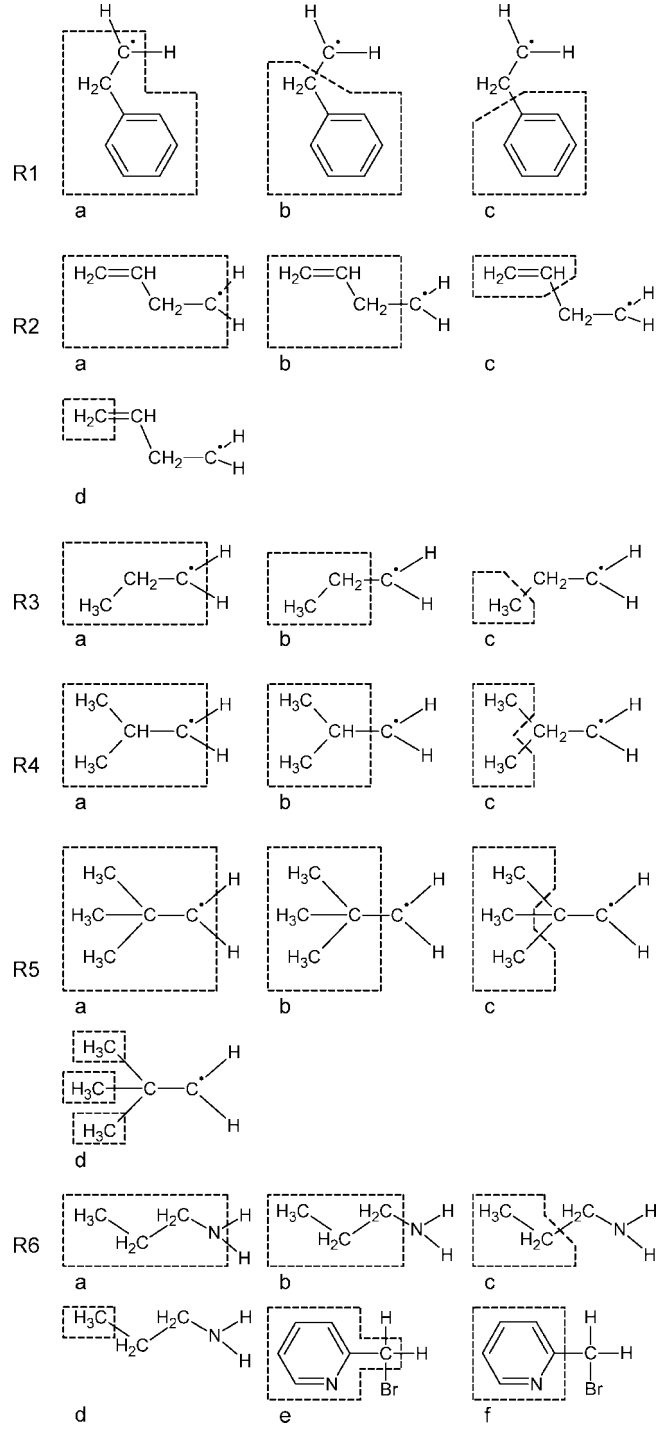

Figure 2. Numbering and choice of the different blocks.

reactants. This case will be denoted as a−b and only makes sense when using MBH.

4. Discussion

4.1. MBH with a Single Block. In the MBH (PHVA) approach, the total partition function of eq 1 is used to calculate the reaction rate, but the vibrational partition function q_{vib} is constructed with the MBH (PHVA) frequencies:

$$q^{\mathrm{MBH}} = q_{\mathrm{trans}} q_{\mathrm{rot}} q_{\mathrm{vib}}^{\mathrm{MBH}} \tag{13}$$

$$q^{\mathrm{PHVA}} = q_{\mathrm{trans}} q_{\mathrm{rot}} q_{\mathrm{vib}}^{\mathrm{PHVA}} \tag{14}$$

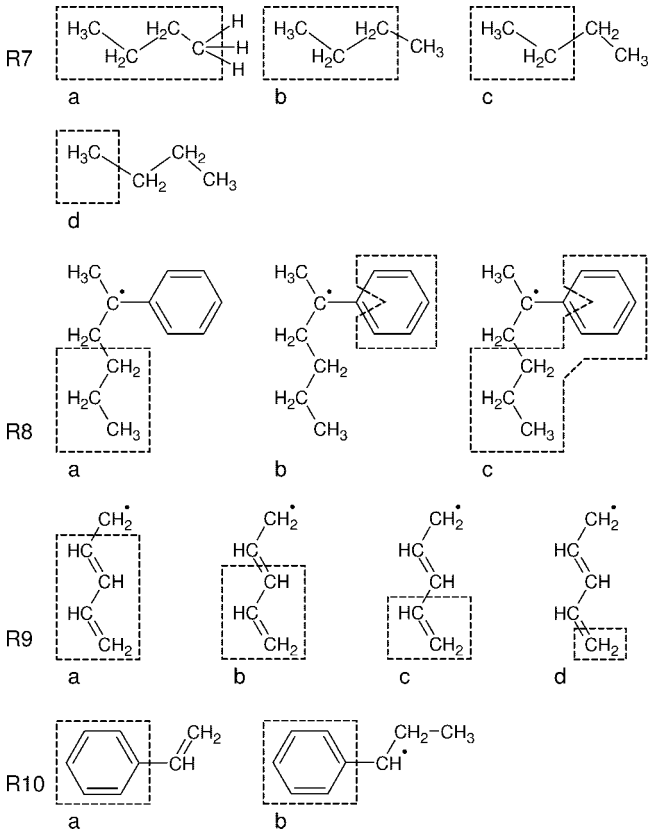

Figure 3. Numbering and choice of the different blocks—continuation.

The chosen test set of chemical reactions allows an exhaustive investigation of the influence on the rate constant of the position of the rigid block, the block's mass, its distance to the reactive center, and the stochiometry of the reaction.

In Tables 1 and 2, the rate constants at $T = 300$ K are listed for the several reactions in units of cubic meters per mole second (bimolecular reactions) or inverse seconds (unimolecular reactions). In the first column, the benchmark values k, calculated with the full Hessian frequencies of the equilibrium structure, are tabulated for comparison. The benchmark is only available for the fully optimized structure and is calculated in absence of any block. The block size in the MBH or PHVA approach applied on a fully optimized structure is indicated by a, b, c etc. A prime is added if the geometry was obtained by partial optimization, e.g. a′, b′, c′, etc.

In a first step, we concentrate on the results obtained with the fully optimized structures. In the next step, the influence of the partial optimization will be discussed.

As can be seen in Tables 1 and 2, the overall agreement of the MBH rate constants with the benchmark values is remarkably good. The reaction rate constants are reproduced to within a factor of 2, apart from a few cases in Table 2, which are discussed further. This observation holds for a variety of reactions: for unimolecular and bimolecular reactions, for radical and nonradical reactions, and for heavy or small block masses. The deviation is within acceptable limits and is smaller than corrections induced by the level of theory,[31] internal rotations,[32,33] tunnel effects, and other factors.[34,35]

The apparent agreement of the MBH predictions with the benchmark implies that the contribution of the omitted normal modes, inherent to the MBH method, is of the same magnitude for both the transition states and reactants. Apparently the omitted modes are not essential in the determination of the rate constant. These rather unimportant modes are localized in the fixed block or spread out over the fixed block and the optimized region. The more interesting modes are located in the optimized region that contains the active site, and are well reproduced by the MBH approach. The coupling of the MBH modes with the modes localized in the fixed block is left out in the model, but a logical choice of the blocks makes this coupling irrelevant for the rate constant.

When a block is chosen too close to the active site, the coupling between MBH modes and the omitted modes is not always irrelevant anymore. In reaction R1 the rigid block a includes the reactive center, and the border of block b crosses the bond connecting the radical center. The reaction rate constant k^{MBH} indeed overestimates the benchmark value. Block c is a better choice because it is not directly connected to the reactive site.

In some particular cases, e.g. reaction R4 with block a or b, the MBH approach reproduces k fairly well even with a direct bond between active site and block. However, one should not rely on such coincidences, and anyway, a more suitable choice of a block further away from the radical center still improves the rate estimate. As a general rule, hereafter referred to as the bond-distance rule, it is recommended not to bring the block region too close to the active site.

The mass of the rigid block does not play a crucial role in the validation of MBH in reproducing rate constants. This is best illustrated by comparing reactions R1 and R2. In R1, the fixed block c contains a phenyl group, while block c in R2 consists of an ethyl group. Results are comparable for both the forward and reverse reactions.

When we finally consider the results of the partial optimization, it is clear that the effect is rather moderate. We concentrate on the forward reaction R1 for a detailed study (Table 3). The partial optimization affects the geometry, because the rigid block conserves its initial internal geometry. This will cause differences with the benchmark geometry. In this simple example, this induces quite slight changes (some C−C distances are increased by 0.03 Å), but in more complex systems, the low level of theory geometry and partial optimized geometry may differ substantially. Or, the full optimization at the low level of theory should give a plausible internal geometry for the blocks, but the exact position/orientation of the blocks and the positions of the relaxed atoms are less important, since these are optimized during the consecutive partial optimization at the high level of theory, giving a plausible geometry of the whole system.

The ground-state configuration of a partially optimized system is obviously less bound than the fully optimized system. However, the energy increase of 2 kJ/mol, noticed in the ethylbenzene radical, is mostly compensated by a similar increase of the binding energy of the TS, hence resulting in an almost equal reaction barrier. For instance,

Table 1. Calculated Rate Constants at $T = 300$ K, for Reactions R1–R4 of the Test Set[a]

	forward					backward				
reaction	k	block	k^{PHVA}/k	k^{PHVA*}/k	k^{MBH}/k	k	block	k^{PHVA}/k	k^{PHVA*}/k	k^{MBH}/k
R1	3.46E−02	a	5.36	1.23	1.36	1.86E−06	a	0.39	0.35	0.48
		b	7.44	1.71	1.74		b	0.91	0.83	0.83
		c	4.33	0.99	1.02		c	1.13	1.02	0.95
		a′	5.97	1.37	1.52		a′	0.37	0.34	0.46
		b′	7.58	1.73	1.76		b′	0.99	0.90	0.90
		c′	4.21	0.96	0.99		c′	1.15	1.04	0.97
R2	2.85E−02	a	10.00	1.00	1.12	1.78E−06	a	0.43	0.36	0.65
		b	14.68	1.47	1.44		b	1.03	0.86	0.88
		c	8.91	0.89	0.93		c	1.09	0.91	0.96
		d	9.62	0.96	1.00		d	1.16	0.96	1.00
		a′	8.31	0.84	0.94		a′	0.40	0.34	0.61
		b′	10.83	1.09	1.07		b′	1.06	0.89	0.92
		c′	8.41	0.84	0.88		c′	1.07	0.89	0.96
		d′	9.62	0.96	1.00		d′	1.16	0.96	1.00
R3	1.47E−02	a	14.68	0.98	1.23	1.51E−06	a	0.44	0.35	0.69
		b	19.84	1.32	1.33		b	1.00	0.81	0.85
		c	14.78	0.98	0.99		c	1.18	0.95	0.99
		a′	16.56	1.10	1.39		a′	0.41	0.33	0.65
		b′	21.08	1.40	1.41		b′	1.06	0.85	0.89
		c′	14.73	0.98	0.99		c′	1.22	0.98	1.03
R4	1.99E−03	a	7.21	0.82	1.10	4.93E−06	a	0.34	0.28	0.61
		b	9.14	1.04	1.09		b	0.75	0.62	0.70
		c	8.66	0.98	0.97		c	1.27	1.05	1.08
		a′	7.52	0.86	1.14		a′	0.28	0.23	0.49
		b′	8.52	0.97	1.01		b′	0.76	0.63	0.71
		c′	8.57	0.97	0.96		c′	1.38	1.14	1.16

[a] The forward rate constants are expressed in units of cubic meters per mole second (bimolecular), and the backward rate constants are in units of inverse seconds (unimolecular). The benchmark value k is given for comparison. Rate constants k^{MBH} (k^{PHVA}, k^{PHVA*}) are calculated with the MBH (PHVA, PHVA*) frequencies, for several block choices. The ratios reflect the influence of the MBH (PHVA, PHVA*) treatment with respect to the benchmark value. A block without a prime indicates a fully optimized structure, and a block with a prime indicates a partially optimized structure.

in the case study, a suitable choice of the fixed block (block c′) predicts a reaction barrier that is hardly different (by 0.04 kJ/mol) from the benchmark value (see Table 3). Significant changes of reaction barriers alter the reaction rate constant to a large extent, but apparently the various reactions R1–R5 of the test set give no indication of this behavior, if one respects sufficient distance between the fixed blocks and the reactive site.

In Table 3, the kinetic parameters A and E_a, determined within the temperature range 300−700 K, are also given. Activation energies remain almost unaffected as could be expected. Potential deviations of k^{MBH} originate from the pre-exponential factor, which is mainly determined by the vibrational contribution to the partition function.

The above discussion validates the use of the MBH model to predict the rate constant on an accurate level. A plausible choice of the fixed block is the only essential ingredient a potential user of MBH should take into account to get adequate predictions of chemical kinetics. MBH is computationally attractive, makes quantum chemical calculations feasible in extended molecular systems, and preserves the true reaction mechanism.

4.2. MBH with Multiple Blocks. The ability of MBH to choose multiple blocks freely moving but conserving their internal structure makes it a powerful tool to a broad range of applications. This is demonstrated in reactions R5, R8, and R10 of the test set, and the results are tabulated in Tables 1 and 2.

In reaction R5, the effect of multiple blocks compared to a single block (block choice d versus c) is moderate. Reaction R8 describes a more complex system. Two individual blocks a and b can be merged to one solid block c, or they can be considered as two mobile blocks a−b. Here, the multiple MBH implies a significant improvement with respect to the single block treatment c. Block c yields ratios 3.86 and 0.44 for the forward and backward reaction, respectively, while the multiple blocks a−b give values of 1.67 and 0.76. Inspection of the MBH values obtained with the individual blocks a and b shows that the global effect of multiple blocks is mostly given by the following multiplication rule:

$$\frac{k_{a-b}^{MBH}}{k} \approx \frac{k_{a}^{MBH}}{k} \times \frac{k_{b}^{MBH}}{k} \tag{15}$$

This seems to be true for the forward and backward reaction.

A third example is reaction R10 where we choose a block in each reactant. The TS will then contain two blocks, which are treated within the multiple MBH. The overall factor is indeed fairly well reproduced by the multiplication rule (14). At least it gives an indication on the global error induced by the presence of multiple blocks. A plausible block choice is always of importance to keep the error within the limits. Unphysical block choices are for example b in R8 and c in R9. In both cases the block's border crosses a bond that is part of a delocalized system, and therefore, the k^{MBH} ratios are badly reproduced, even when the bond-distance rule is respected.

Table 2. Calculated Rate Constants at $T = 300$ K, for Reactions R5–R10 of the Test Set[a]

	forward					backward				
reaction	k	block	k^{PHVA}/k	k^{PHVA*}/k	k^{MBH}/k	k	block	k^{PHVA}/k	k^{PHVA*}/k	k^{MBH}/k
R5	1.72E−03	a	5.46	0.84	1.01	2.94E−06	a	0.42	0.36	0.60
		b	6.57	1.01	1.04		b	0.91	0.77	0.85
		c	6.28	0.96	0.99		c	1.03	0.88	0.95
		d			1.04		d			0.98
		a′	6.12	0.94	1.13		a′	0.43	0.36	0.61
		b′	6.47	0.99	1.03		b′	1.07	0.91	0.99
		c′	6.46	0.99	1.01		c′	1.19	1.01	1.08
		d′			1.16		d′			1.23
R6	9.93E−12	a	1060.01	1.74	1.76	1.41E−13	a	0.51	0.49	0.69
		b	1002.56	1.64	1.71		b	0.81	0.78	0.78
		c	794.07	1.30	1.33		c	0.89	0.86	0.85
		d	657.28	1.08	1.10		d	1.11	1.08	1.00
		e	2.61	0.29	0.85		e	0.17	0.16	0.56
		f	8.70	0.96	1.00		f	0.83	0.80	0.80
R7	2.85E+07	a	4.15	0.43	0.95	1.24E−04	a	10.67	2.03	1.73
		b	4.66	0.49	0.99		b	8.37	1.59	1.56
		c	4.86	0.51	1.05		c	5.50	1.04	1.02
		d	4.79	0.50	1.03		d	5.41	1.03	1.02
		a′	5.06	0.53	1.16		a′	16.69	3.19	2.71
		b′	5.22	0.55	1.11		b′	9.74	1.84	1.82
		c′	5.03	0.52	1.08		c′	5.58	1.06	1.04
		d′	4.85	0.51	1.04		d′	5.48	1.04	1.04
R8	8.04E−11	a	2.14	1.14	1.11	2.97E+02	a	1.31	1.25	0.99
		b	3.01	1.61	1.50		b	0.89	0.84	0.77
		c	5.91	3.15	3.86		c	0.48	0.46	0.44
		a−b			1.67		a−b			0.76
R9	1.83E−09	a	21.89	2.53	2.64	3.27E+01	a	1.60	1.31	2.27
		b	14.00	1.62	1.50		b	0.99	0.81	1.29
		c	14.40	1.66	1.63		c	2.29	1.87	5.14
		d	10.24	1.18	0.98		d	0.69	0.57	2.04
R10	3.02E−06	a	43.51	0.89	0.96					
		b	30.18	1.34	1.59					
		a−b			1.53					

[a] See the footnote of Table 1 for more details.

Table 3. MBH for Reaction R1 with Fully and Partially Optimized Structures[a]

	full optim			partial optim		
	a	b	c	a′	b′	c′
k^{MBH}/k	1.36	1.74	1.02	1.52	1.76	0.99
A^{MBH}/A	1.29	1.59	1.03	1.38	1.70	1.01
$E_a^{MBH} - \Delta E_a$	−0.14	−0.21	0.01	−0.22	−0.02	+0.06
$\Delta E_0^{MBH} - \Delta E_0$	0	0	0	−0.13	+0.13	+0.04

[a] The rate constant is given at 300 K, and kinetic parameters are fitted in the temperature range 300–700 K. k and A are in cubic meters per mole second, and energies are in kilojoules per mole. Benchmark values: $k = 3.46 \times 10^{-2}$ m^3 mol^{-1} s^{-1}, $A = 67.22 \times 10^2$ m^3 mol^{-1} s^{-1}, $E_a = 36.53$ kJ/mol, $\Delta K_0 = 24.66$ kJ/mol.

4.3. MBH for Modeling Solvents. Finally, we have tested the concept of multiple blocks on a more realistic and more extended example, where several explicit solvent molecules are taken into account in the computation. In this case, blocks can be chosen within the reacting molecule and/or the solvent molecules can be treated as blocks, and moreover, the influence of solvent species on both reaction barrier and frequencies, i.e. pre-exponential factor, can be tested.

We have chosen the cyclization of functionalized aminophosphonates, as a representative reaction occurring in an organic solvent (reaction R11, see Figure 4). The choice of this reaction was inspired by a recent combined experimental and theoretical study on the formation of β-lactams by some

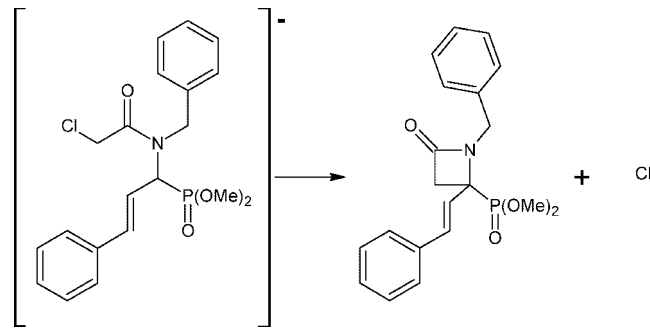

Figure 4. Reaction R11.

of the authors.[36] It was found that, starting from an ambient allylic anion, ring closure occurred exclusively by 4-ring formation, without any trace of 6-ring lactams. At that time, pre-exponential factors were not calculated due to the high computational cost. This is thus an ideal example to validate the approach.

The studied system consists of the aminophosphonate anion together with a sodium counterion and solvated in dimethyl ether solvent molecules (DME). The latter were taken as model molecules for tetrahydrofuran. Three cases are considered: the reaction in the absence of explicit solvent molecules (R11), in the presence of one DME (R11 + 1DME), and in the presence of two DMEs (R11 + 2DME). The benchmark values of k, A, E_a, and ΔE_0 are given in Table 4 for $T = 300$ K. The ratios (for k and A) and differences

Table 4. Benchmark Results for Reaction R11 without and with 1 and 2DME[a]

	R11	R11 + 1DME		R11 + 2DME	
k	7.62E−15	6.79E−14	(8.91)	2.09E−12	(274.63)
A	2.10E+13	8.43E+12	(0.40)	5.64E+13	(2.69)
E_a	157.73	149.99	(−7.73)	146.19	(−11.54)
ΔE_0	159.85	151.78	(−8.07)	148.23	(−11.63)

[a] The rate constant is given at 300 K, and kinetic parameters are fitted in the temperature range 300–700 K. k and A are in inverse seconds, and energies are in kilojoules per mole. Ratios (k and A) and differences (E_a and ΔE_0) between solvated and nonsolvated values are given between brackets.

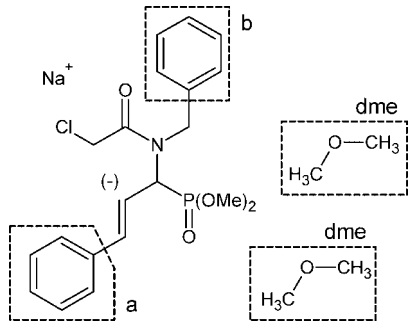

Figure 5. Definition of blocks, reaction R11.

Table 5. Calculated at 300 K[a]

block	R11	R11 + 1DME	R11 + 2DME
a	1.71	1.62	1.43
b	0.98	0.97	0.88
dme		1.07	
b−dme		1.04	
dme−dme			0.94
b−dme−dme			0.83

[a] Several blocks choices are taken up.

(for energies) given between brackets indicate the effect of the solvation. The presence of one or two solvent molecules indeed increases the reaction rate constant by a factor of 8.91 or 274.63, respectively, with respect to the nonsolvated situation.

The relevant question is whether the MBH model is capable of reproducing the enhancement of k due to the solvent. Several block choices are depicted in Figure 5, including the case of blocks within the reactant (a, b), as well as blocks consisting of solvent molecules (dme). Table 5 shows the ratios between the MBH estimates and the benchmark values of the rate constant. Block a is clearly not a good choice, which is easily understood when noting that the block's border cuts through a delocalized bond. Therefore, possible combinations of a with blocks b or dme are not considered in the table. Block b and block dme on the other hand are excellent block choices: since the ratios are close to 1.0, the k enhancement 1:8.91:274.63 as reported by the benchmark is maintained and the MBH is thus clearly capable of reproducing the solvation effect. Multiple block combinations such as b−dme, dme−dme, and b−dme−dme reproduce the rate constant very well, which is in agreement with the multiplication rule as stated in eq 14. Resuming, the multiple MBH has proven to be extremely useful and effective in predicting reaction rates, both with blocks belonging to the reactant or with blocks coinciding with solvent molecules.

4.4. PHVA and PHVA*. Conceptually, the difference between MBH and PHVA is mainly a mass effect. In the MBH, the finite mass of the blocks is taken into consideration, while in the PHVA approach, infinite masses are associated with the atoms in the rigid body. As a result, an extension to multiple blocks has no physical meaning in PHVA. When two blocks with infinite mass are present within one molecule, the system of free atoms and blocks will behave as if the two blocks were one big block with infinite mass. The case of one block in each of the reactants of a bimolecular reaction must also be excluded. The transition state itself would have two blocks with infinite mass. Thereby, six degrees of freedom describing the relative position and orientation of the two blocks will be lost in the transition state, leading to a completely wrong temperature dependence of the reaction rate constant. From a physical point of view, it is also hard to imagine how two reactants, each containing a block with infinite mass, could ever approach each other to form the transition state. The following discussion is therefore limited to the case of a single block with fixed geometry.

In contrast to the MBH, the PHVA cannot be extended to treat multiple blocks. PHVA is thus only applicable within the single block approximation. An overview of the various PHVA reaction rates in Tables 1 and 2 shows that unimolecular reactions are reasonably well described using PHVA frequencies. On the other hand, bimolecular reaction rates are poorly reproduced and significant deviancies are noticed. The systematic overestimation of the reaction rate finds its origin in the appearance of spurious low frequency modes in the PHVA approach. A profound investigation of these spurious modes reveals that they represent slow translation/rotationlike movements of the whole group of free atoms. This collective motion encompasses a lot of mass, explaining why (through the mass weighting in the NMA analysis) these frequencies are low. They give a significant contribution to the vibrational partition functions, while the translational/rotational degrees of freedom, however, are already taken into account in the total partition function. The larger the total mass of the free atoms with respect to the mass of the fixed block, the more pronounced is this double counting. Hence, in unimolecular reactions, the enhancement of the vibrational partition functions due to this double counting effect is nearly similar for reactant and transition state, and the enhancement factor is canceled (see eq 8). In bimolecular reactions on the other hand, the double counting is much more prominent for the transition state than for the reactants, thus leading to an overestimated reaction rate.

In order to prevent this double counting effect, we present a corrected version of the PHVA method. In Figure 6, the ratio $q_{vib}^{MBH}/q_{vib}^{PHVA}$ between the MBH and PHVA vibrational partition functions for the reactants, TS, and products of reactions R1–R6 is plotted against a mass related factor t given by

$$t = \sqrt{\frac{M_F^3 I_{F1} I_{F2} I_{F3}}{M^3 I_1 I_2 I_3}} \tag{16}$$

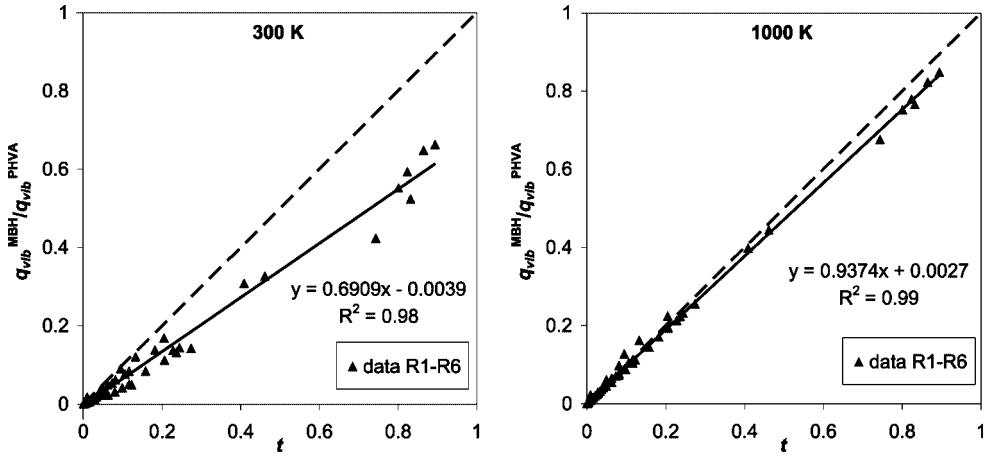

Figure 6. Ratio $q_{vib}^{MBH}/q_{vib}^{PHVA}$ for reactants, TS, and products of reactions R1– R6 plotted against the mass related factor t at 300 and 1000 K. The linear regression line (full) is fitted to the data with the least-squares method. The diagonal (dashed line) is added for comparison.

where M is the total mass and I_i ($i = 1, 2, 3$) are the moments of inertia of the molecule, while M_F and I_{Fi} ($i = 1, 2, 3$) are the total mass and moments of inertia of the fixed block. For higher temperatures, an almost linear behavior is observed.

$$\frac{q_{vib}^{MBH}}{q_{vib}^{PHVA}} \approx t \tag{17}$$

On the basis of eq 17, we now propose the following corrected PHVA partition function, hereafter referred to as PHVA*,

$$q^{PHVA*} = q_{trans} q_{rot} q_{vib}^{PHVA} \sqrt{\frac{M_F{}^3 I_{F1} I_{F2} I_{F3}}{M^3 I_1 I_2 I_3}} \tag{18}$$

It is not surprising that the ratio $q_{vib}^{MBH}/q_{vib}^{PHVA}$ depends only on mass properties, because the essential difference between the MBH and PHVA approach is a reduced mass effect. The plot in Figure 6 is so overwhelming that a mathematical proof of eq 16 should be on hand and that a close similarity between PHVA* and MBH predictions for the reaction rate constants is expected. The latter is indeed confirmed by the corrected PHVA* estimates taken up in Tables 1 and 2. Concluding, PHVA* and MBH perform equally well, but the main advantage of MBH, i.e. enabling the extension the procedure to multiple blocks, still holds.

In the following, a mathematical derivation of eq 17 will be presented. In the high temperature limit ($k_B T >> h\nu$, $\forall \nu$), it is possible to relate q_{vib}^{PHVA} and q_{vib}^{MBH} as a simple expression containing ratios of the masses and moments of inertia. The contribution of a vibration with frequency ν to the partition function is given by eq 5 and can be approximated by $k_B T/h\nu$ if the temperature is high with respect to the vibrational temperature $h\nu/k_B$. Since the number of MBH and PHVA frequencies is equal, the ratio is independent of temperature.

$$\frac{q_{vib}^{MBH}}{q_{vib}^{PHVA}} = \frac{\Pi_\nu \nu^{PHVA}}{\Pi_\nu \nu^{MBH}} \tag{19}$$

The product of frequencies coincides with the square root of the determinant of the matrix in the NMA normal mode equations. In the PHVA model (eq 10), this is

$$\prod_\nu \nu^{PHVA} = \sqrt{\det(M_E{}^{-1/2} H_E M_E{}^{-1/2})} \tag{20}$$

while in the MBH model (eq 11), this is

$$\prod_\nu \nu^{MBH} = \sqrt{\det(\tilde{M}'^{-1/2} H_E \tilde{M}'^{-1/2})} \tag{21}$$

The ratio becomes

$$\frac{q_{vib}^{MBH}}{q_{vib}^{PHVA}} = \sqrt{\frac{\det \tilde{M}'}{\det M_E}} \tag{22}$$

We now introduce the matrix S, defined in the Appendix, which contains the mass information of the complete system. Eigenvalues are the total mass M and the moments of inertia I_i. Similarly we introduce the matrix S_F for the fixed atoms, with eigenvalues M_F and I_{Fi}. Using the properties described in ref 17, the ratio can be rewritten (see the Appendix):

$$\frac{q_{vib}^{MBH}}{q_{vib}^{PHVA}} = \sqrt{\frac{\det S_F}{\det S}} \tag{23}$$

which is equivalent to expression 17 and which proves the PHVA* correction factor of eq 18.

Numerically, we find that eq 18 is not only valid for high temperatures but that its validity holds quite well for lower temperatures (300 K); see Figure 6.

An interesting property is that the mass related factor t of eq 16 is also equal to the ratio of the translational/rotational partition functions of the fixed block versus global molecule

$$\sqrt{\frac{M_F{}^3 I_{F1} I_{F2} I_{F3}}{M^3 I_1 I_2 I_3}} = \frac{q_{F,trans} q_{F,rot}}{q_{trans} q_{rot}} \tag{24}$$

The subscript F refers to the fixed block atoms. Thus, an alternative formulation of the PHVA* approach is presented, where only the vibrational partition function is taken into account. The total translational and rotational partition

function of the molecule are omitted as if it were to avoid the double counting effect.

$$q^{\mathrm{PHVA}*} = q_{\mathrm{vib}}^{\mathrm{PHVA}} \tag{25}$$

Expression 25 is different from the one proposed in eq 17, but it amounts to the same result when calculating reaction rates. The factor $M_{\mathrm{F}}{}^{3/2}$ is the same in both TS and reactants because the same block atoms are chosen, and thus, this factor is canceled in the numerator and denominator in the expression of k. The factor $\sqrt{I_{\mathrm{F1}}I_{\mathrm{F2}}I_{\mathrm{F3}}}$ might slightly differ between TS and reactants, if the internal geometry of the blocks is not completely identical for the TS and reactants, but in good approximation, it is canceled as well. The factor $M^{3/2}$ cancels with the translational partition function and $\sqrt{I_1I_2I_3}$ with the vibrational partition function. Therefore, eq 25 will lead to (almost) identical results as eq 17.

5. Conclusion

In this work, the MBH method has been shown to act as an accurate method for the prediction of chemical kinetics in large extended molecular systems. In contrast to the PHVA approach, the MBH method also performs fairly well in bimolecular reactions. An adapted version of PHVA is presented correcting for the double counting effect of global rotation and translation inherent to the PHVA method. The surplus value of MBH with regard to PHVA* lies in the flexibility of MBH to introduce multiple rigid blocks which are freely moving with respect to each other but keeping their initial internal structure. This facility gives a lot of new perspectives in predicting chemical kinetics in very complex systems, where the introduction of one single fixed block is a too crude approximation. Partial optimization is necessary to make quantum chemical computations feasible. The possibility to introduce multiple blocks, each still having six degrees of freedom, makes an accurate reproduction of kinetics to the possibilities.

Most promising application field of MBH would be the description of chemical reactions in a solvent. Each solvent molecule may be regarded as a fixed block, keeping its internal structure, but still enabling to translate/rotate freely with respect to the chemically active part of the system. All ab initio program packages can be used on the condition that the built-in optimization routine allows constraints on internal degrees of freedom. The computational advantage of the MBH method can be exploited when the program package has the ability to calculate partial Hessians. If both features are implemented, MBH could be regarded as a groundbreaking model in the treatment of complex reactions where environment plays a crucial role.

Acknowledgment. This work is supported by the Fund for Scientific Research−Flanders and by the BOF funds of Ghent University.

Appendix

Consider a molecule with N masses m_A, $A = 1, \ldots, N$. The positions are described by Cartesian coordinates $\mathrm{r}_A \equiv \{r_{A\mu}\}_{\mu=x,y,z}$, with respect to a space-fixed frame. We will treat the case of one MBH block, consisting of N_{F} atoms. The remaining $N_{\mathrm{E}} = N - N_{\mathrm{F}}$ atoms are in equilibrium due to the partial optimization. An index E (F) will be used to indicate quantities where only the free (fixed) atoms are considered.

We will focus on the normal mode equations for PHVA and for MBH and, in particular, on the difference in the mass matrices, in order to study the transition from eq 22 to eq 23. The PHVA mass matrix is simply given by M_{E} [see ()]. The original (not yet transformed to (11)) MBH normal mode equations read

$$\tilde{H}\nu = \lambda\tilde{M}\nu \tag{26}$$

where $\tilde{M}$ and $\tilde{H}$ are the MBH mass matrix and Hessian [see ref 17].

Define now a $3N \times 6$ matrix D with components

$$D_{A\mu,\,\alpha} = \begin{cases} \delta_{\mu,x} & \alpha = 1 \\ \delta_{\mu,y} & \alpha = 2 \\ \delta_{\mu,z} & \alpha = 3 \\ \Sigma_\lambda \epsilon_{\lambda\mu x} & \alpha = 4 \\ \Sigma_\lambda \epsilon_{\lambda\mu y} & \alpha = 5 \\ \Sigma_\lambda \epsilon_{\lambda\mu z} & \alpha = 6 \end{cases} \tag{27}$$

With M as the diagonal $3N \times 3N$ mass matrix, the matrix $S = D^{\mathrm{T}}MD$ is introduced, and similarly, $S_{\mathrm{F}} = D_{\mathrm{F}}{}^{\mathrm{T}}M_{\mathrm{F}}D_{\mathrm{F}}$. The MBH mass matrix is then given by the block diagonal matrix

$$\tilde{M} = \begin{pmatrix} S_{\mathrm{F}} & 0_{6\times d} \\ 0_{d\times 6} & M_{\mathrm{E}} \end{pmatrix} \tag{28}$$

with $d = 3N_{\mathrm{E}}$. The normal mode equations are transformed by simultaneous block diagonalization of $\tilde{H}$ and $\tilde{M}$. The required transformation matrices are given by

$$T_1 = \begin{pmatrix} 1_{6\times 6} & 0_{6\times d} \\ x & 1_{d\times d} \end{pmatrix}; \quad T_2 = \begin{pmatrix} 1_{6\times 6} & y \\ 0_{d\times 6} & 1_{d\times d} \end{pmatrix} \tag{29}$$

with $x = D_{\mathrm{E}}$ and $y = -S^{-1}D_{\mathrm{E}}{}^{\mathrm{T}}M_{\mathrm{E}}$. The transformed MBH mass matrix and Hessian directly lead to eq 11:

$$T_2^{\mathrm{T}}T_1^{\mathrm{T}}\tilde{H}T_1T_2 = \begin{pmatrix} 0_{6\times 6} & 0_{6\times d} \\ 0_{d\times 6} & H_{\mathrm{E}} \end{pmatrix}, \quad T_2^{\mathrm{T}}T_1^{\mathrm{T}}\tilde{M}T_1T_2 = \begin{pmatrix} S & 0_{6\times d} \\ 0_{d\times 6} & \tilde{M}' \end{pmatrix} \tag{30}$$

with $\tilde{M}' = M_{\mathrm{E}} - M_{\mathrm{E}}D_{\mathrm{E}}S^{-1}D_{\mathrm{E}}{}^{\mathrm{T}}M_{\mathrm{E}}$. Or, the relevant mass matrix is $\tilde{M}'$ for MBH.

Since by construction $\det T_1 = \det T_2 = 1$, it is obvious that the following relations between determinants hold:

$$\det \tilde{M} = \det S_{\mathrm{F}} \det M_{\mathrm{E}} \tag{31}$$

$$\det (T_2^{\mathrm{T}}T_1^{\mathrm{T}}\tilde{M}T_1^{\mathrm{T}}T_2^{\mathrm{T}}) = \det \tilde{M} = \det S \det \tilde{M}' \tag{32}$$

or

$$\frac{\det \tilde{M}'}{\det M_{\mathrm{E}}} = \frac{\det S_{\mathrm{F}}}{\det S} \tag{33}$$

This proves the transition between eqs 22 and 23.

References

(1) Gao, J. L.; Truhlar, D. G. *Annu. Rev. Phys. Chem.* **2002**, *53*, 467–505.

(2) Eyring, H. *J. Chem. Phys.* **1935**, *3*, 107.

(3) Evans, M. G.; Polanyi, M. *Trans. Faraday Soc.* **1935**, *31*, 875.

(4) Laidler, K. J. *Chemical Kinetics*; Harper Collins Pulbishers, Inc.: New York, 1987, 87–138..

(5) Mc Quarrie, D. A.; Simon, J. D. *Physical Chemistry - a molecular approach*; University Science Books: Sausalito, CA, 1997; pp 1075–1079..

(6) Warshel, A.; Levitt, M. J. *Mol. Biol.* **1976**, *103* (2), 227–249.

(7) Assfeld, X.; Rivail, J. L. *Chem. Phys. Letters* **1996**, *263* (1–2), 100–106.

(8) Gao, J. L.; Amara, P.; Alhambra, C.; Field, M. J. *J. Phys. Chem. A* **1998**, *102* (24), 4714–4721.

(9) Zhang, Y. K.; Lee, T. S.; Yang, W. T. *J. Chem. Phys.* **1999**, *110* (1), 46–54.

(10) Ghysels, A.; Van Neck, D.; Van Speybroeck, V.; Verstraelen, T.; Waroquier, M. *J. Chem. Phys.* **2007**, *126* (22), 224102.

(11) Jin, S. Q.; Head, J. D. *Surf. Sci.* **1994**, *318* (1–2), 204–216.

(12) Calvin, M. D.; Head, J. D.; Jin, S. Q. *Surf. Sci.* **1996**, *345* (1–2), 161–172.

(13) Head, J. D. *Int. J. Quantum Chem.* **1997**, *65* (5), 827–838.

(14) Head, J. D. *Int. J. Quantum Chem.* **2000**, *77* (1), 350–357.

(15) Li, H.; Jensen, J. H. *Theor. Chem. Acc.* **2002**, *107*, 211–219.

(16) Besley, N. A.; Metcalf, K. A. *J. Chem. Phys.* **2007**, *126* (3), 035101.

(17) Ghysels, A.; Van Neck, D.; Waroquier, M. *J. Chem. Phys.* **2007**, *127*, 164108.

(18) Lin, H.; Pu, J. Z.; Albu, T. V.; Truhlar, D. G. *J. Phys. Chem. A* **2004**, *108* (18), 4112–4124.

(19) Garcia-Viloca, M.; Alhambra, C.; Truhlar, D. G.; Gao, J. *J. Chem. Phys.* **2001**, *114* (22), 9953–9958.

(20) Fernandez-Ramos, A.; Miller, J. A.; Klippenstein, S. J.; Truhlar, D. G. *Chem. Rev.* **2006**, *106* (11), 4518–4584.

(21) Stevens, F.; Vrielinck, H.; Van Speybroeck, V.; Pauwels, E.; Callens, F.; Waroquier, M. *J. Phys. Chem. B* **2006**, *110* (16), 8204–8212.

(22) Lesthaeghe, D.; Delcour, G.; Van Speybroeck, V.; Marin, G.; Waroquier, M. *Microporous Mesoporous Mater.* **2006**, *96*, 350−356.

(23) Lesthaeghe, D.; De Sterck, B.; Van Speybroeck, V.; Marin, G. B.; Waroquier, M. *Angew. Chem., Int. Ed.* **2007**, *46* (8), 1311–1314.

(24) Cui, Q. *J. Chem. Phys.* **2002**, *117* (10), 4720.

(25) Tomasi, J.; Mennucci, B.; Cammi, R. *Chem. Rev.* **2005**, *105* (8), 2999–3093.

(26) Tachibana, A.; Fukui, K. *Theor. Chim. Acta* **1978**, *49* (4), 321–347.

(27) Murry, R.; Fourkas, J. T.; Wu-Xiong, L.; Keyes, T *J. Chem. Phys.* **1999**, *110*, 10410–10422.

(28) Wales, D. J. *J. Chem. Phys.* **2000**, *113*, 3926–3927.

(29) Yang, L. J.; Tan, C. H.; Hsieh, M. J.; Wang, J. M.; Duan, Y.; Cieplak, P.; Caldwell, J.; Kollman, P. A.; Luo, R. *J. Phys. Chem. B* **2006**, *110* (26), 13166–13176.

(30) Frisch, M. J.; Trucks, G. W.; Schlegel, H. B.; Scuseria, G. E.; Robb, M. A.; Cheeseman, J. R.; Montgomery, J. A., Jr.; Vreven, T.; Kudin, K. N.; Burant, J. C.; Millam, J. M.; Iyengar, S. S.; Tomasi, J.; Barone, V.; Mennucci, B.; Cossi, M.; Scalmani, G.; Rega, N.; Petersson, G. A. Nakatsuji, H.; Hada, M.; Ehara, M.; Toyota, K.; Fukuda, R.; Hasegawa, J.; Ishida, M.; Nakajima, T.; Honda, Y.; Kitao, O.; Nakai, H.; Klene, M.; Li, X.; Knox, J. E.; Hratchian, H. P.; Cross, J. B.; Bakken, V.; Adamo, C.; Jaramillo, J.; Gomperts, R.; Stratmann, R. E. ; Yazyev, O.; Austin, A. J.; Cammi, R.; Pomelli, C.; Ochterski, J. W.; Ayala, P. Y.; Morokuma, K.; Voth, G. A.; Salvador, P.; Dannenberg, J. J.; Zakrzewski, V. G.; Dapprich, S.; Daniels, A. D.; Strain, M. C.; Farkas, O.; Malick, D. K.; Rabuck, A. D.; Raghavachari, K.; Foresman, J. B.; Ortiz, J. V.; Cui, Q.; Baboul, A. G.; Clifford, S.; Cioslowski, J.; Stefanov, B. B.; Liu, G.; Liashenko, A.; Piskorz, P.; Komaromi, I.; Martin, R. L.; Fox, D. J.; Keith, T.; Al-Laham, M. A.; Peng, C. Y.; Nanayakkara, A.; Challacombe, M.; Gill, P. M. W.; Johnson, B.; Chen, W.; Wong, M. W.; Gonzalez, C.; Pople, J. A. *Gaussian 03*, revision C.02; Gaussian, Inc.: Wallingford, CT, 2004.

(31) Van Speybroeck, V.; Van Cauter, K.; Coussens, B.; Waroquier, M. *Chemphyschem* **2005**, *6* (1), 180–189.

(32) Van Speybroeck, V.; Van Neck, D.; Waroquier, M. *J. Phys. Chem. A* **2000**, *104* (46), 10939–10950.

(33) Vansteenkiste, P.; Van Neck, D.; Van Speybroeck, V.; Waroquier, M. *J. Chem. Phys.* **2006**, *124* (4), 044314.

(34) Sabbe, M. K.; Saeys, M.; Reyniers, M. F.; Marin, G. B.; Van Speybroeck, V.; Waroquier, M. *J. Phys. Chem. A* **2005**, *109* (33), 7466–7480.

(35) Sabbe, M. K.; Vandeputte, A. G.; Reyniers, M. F. O.; Van Speybroeck, V.; Waroquier, M.; Marin, G. B. *J. Phys. Chem. A* **2007**, *111* (34), 8416–8428.

(36) Van Speybroeck, V.; Moonen, K.; Hemelsoet, K.; Stevens, C. V.; Waroquier, M. *J. Am. Chem. Soc.* **2006**, *128* (26), 8468–8478.

CT7002836